AIAA JOURNAL
Vol. 37, No. 12, December 1999

Effect of Compressible Flow on Perceived Temperature Fluctuations Measured by Moving Sensor

George Y. Jumper,* Robert R. Beland,† John R. Roadcap,‡ and Owen R. Coté§
U.S. Air Force Research Laboratory, Hanscom Air Force Base, Massachusetts 01731-3010

Equations are developed for the effect of velocity fluctuations on a moving temperature sensor. The impact of these fluctuations on perceived fluctuations of the index of refraction is computed. The magnitude of this effect is estimated using known ranges of fluctuations in atmospheric temperature and velocity. By the use of a method to estimate velocity fluctuations from temperature fluctuations and concurrently measured atmospheric data, balloon derived fluctuation data are used to estimate the perceived fluctuations of a faster moving sensor. We conclude that normally observed velocity fluctuations, if uncorrected, can have a significant impact on the perceived optical properties in the troposphere for higher velocity temperature sensors.

Nomenclature

a = constant or coefficient
$B_r(x)$ = spatial covariance (units of r^2)
b = constant or coefficient
C_p = specific heat at constant pressure, J/kg/K
C_x^2 = structure constant of the quantity x (units of $x^2/m^{2/3}$)
$D_x(r)$ = structure function of quantity x (units of x^2)
d = distance, m
g = acceleration of gravity, m/s^2
i, j, k = unit vectors (with caret)
k = spatial wave number, m^{-1}
n = nondimensional index of refraction
P = pressure or partial pressure when subscripted, Pa
r = nondimensional recovery factor; see Eq. (2)
$S_x(k)$ = one-sided, one-dimensional spatial power spectrum of x
T = temperature, K
$\boldsymbol{U}$ = true air speed vector, m/s
u, v, w = components of wind velocity, W to E, S to N, and upward, respectively, m/s
$\boldsymbol{V}$ = velocity vector, m/s
x = distance, m
Z = altitude in plots, km
z = distance in vertical direction, m
γ = ratio of specific heat at constant pressure to specific heat at constant volume
ε = turbulent kinetic energy dissipation rate, W kg^{-1} or m^2 s^{-3}
θ = potential temperature, K; see Eq. (21)
λ = wavelength of refracted radiation, m
χ = dissipation rate of temperature variance, K^2 s^{-1}

Subscripts

d = dry air
gs = ground speed
n = index of refraction
r = recovery
T = temperature
U or u = velocity
w = wind
wv = water vapor
1, 2 = location 1 or 2

Superscripts

$\bar{}$ = time-averaged or mean component
$'$ = fluctuating component

Introduction

OPTICAL turbulence in the atmosphere is defined as fluctuations of the index of refraction, both in space and time. Whereas it is most obviously manifested by the twinkling of stars, it also is a major source of performance degradation for optical systems. For instance, in the presence of optical turbulence, a projected beam appears to wander, broaden, and scintillate, thereby reducing image quality and effectively reducing the average power that arrives at a spot. Optical turbulence is caused by the presence of adjacent parcels of air, at slightly different index of refraction, moving about in the path of propagating electromagnetic waves.

The index of refraction, n, in the atmosphere can be written as[1]

$$n - 1 = a_d(\lambda) P_d/T + a_{\mathrm{wv}}(\lambda) P_{\mathrm{wv}}/T \tag{1}$$

where P is the partial pressure of either the dry air d or the water vapor wv and the a coefficients are the wavelength-dependent coefficients for either the dry air or the water vapor. Fluctuations in the index of refraction are caused by fluctuations of the density of the air, of the concentration of water vapor in the air, or of both.[2] For radiation in the visible and near infrared (IR), the coefficient of the water vapor term is so small that it hardly contributes to the index of refraction, except, perhaps, at very low altitudes over a body of water. Fluctuations in index of refraction can be measured optically over a path with instruments such as a scintillometer. Radars detect fluctuations in the index of refraction of the view volume by Bragg scatter (Ref. 3, p. 115). At microwave frequencies, the index of refraction is much more sensitive to water vapor; therefore, radar results must be corrected when applied to optical and near IR systems. Although both pressure and temperature appear in Eq. (1), fluctuations in pressure are small, they dissipate rapidly through acoustic processes, and the sensitivity of Eq. (1) to changes in pressure is only 1% of the sensitivity to changes in temperature. Therefore, in situ measurement of optical turbulence is, in practice, reduced to measurement of fluctuations in temperature.

Fine-scale, wire temperature sensors carried aloft by balloons and aircraft have been used for in situ measurement of temperature fluctuations. These platforms complement each other to provide a more complete picture of the atmosphere. Each balloon-borne sensor passes through only a small portion of the atmosphere at any altitude, whereas a sensor on an airplane can easily probe the horizontal dimension. Measurements have shown that the turbulent

Presented as Paper 98-2830 at the AIAA 29th Plasmadynamics and Lasers Conference, Albuquerque, NM, 15–18 June 1998; received 13 October 1998; revision received 1 June 1999; accepted for publication 7 June 1999.

*Senior Aerospace Engineer, Battlespace Environment Division. Associate Fellow AIAA.
†Senior Research Physicist, Battlespace Environment Division.
‡Senior Scientist, Battlespace Environment Division.
§Research Physicist, Battlespace Environment Division.

layers are much larger in the horizontal dimension than the vertical.[4] Balloons pass through the thin layers typically at about 5 m/s, so that there are concerns about statistical sampling sufficiency. The time that an airborne platform can sample the larger horizontal direction is only limited by the aircraft speed (typically from 100 to over 200 m/s) and the horizontal dimension of a homogeneous portion of the atmosphere, which is still uncertain. Whereas aircraft are limited to a maximum altitude of around 15 km, balloons normally ascend to around 30 km, where the low atmospheric density causes the probes to lose sensitivity due to heat transfer considerations. Whereas aircraft are typically restricted to certain discrete altitudes, a balloon provides continuous sampling of turbulence with height. Upon recognition that balloon-borne turbulence measurements were systematically higher in the daytime than at night, it was concluded that intermittent and uneven solar heating of the two probes was contaminating daytime readings. The single aircraft wire probes are stiffer, and they have not exhibited any diurnal bias.

Whereas both aircraft and balloon-borne temperature sensors are often fine-wire resistance probes, the approaches to the determination of optical turbulence from these instruments are distinctly different. Because the balloon payloads are usually not recoverable, economic considerations have strongly influenced the design of the Thermosonde, the most widely used balloon-borne optical turbulence sensor.[5,6] Two wire probes, spaced 1 m apart on a horizontal boom, sense temperature differences. The probes use 3.45-μm-diam wire that has a time constant of less than 1 ms at nominal ascent speeds and sea level conditions. The temperature difference is continuously averaged by an onboard analog rms integrated circuit. The output of the rms chip is transmitted back to the ground station at 1.2-s intervals. Because the balloon-borne payload is attached to a meteorological radiosonde, concurrent wind velocity, pressure, mean temperature, and humidity information are also relayed to the ground station.

Because aircraft return to base, their optical turbulence sensing approach has evolved in a different direction. Temperature fluctuation data, sensed by a single probe, are collected and stored at high rates. Procedures developed by Otten,[7] Otten et al.,[8] and Otten and Rose[9] have evolved to the use of 5-μm-diam wire probes mounted on a sting at a forward location on the aircraft, where the local pressure is approximately the freestream pressure. The probe signal is divided into mean and fluctuating components and is recorded at 12 kHz (Ref. 10). After the flight, turbulence levels are determined by analysis of the spectrum of short segments of the flight. Airborne measurements are typically made at several nearly constant altitudes over ranges of tens to hundreds of kilometers.

Because the desired state variable is freestream air temperature, one very important consideration is the ability of any temperature sensor to measure fluid temperature while moving relative to the fluid. This is a classic heat transfer problem faced by anyone trying to measure temperature in a moving stream. To achieve maximum sensitivity to temperature, the wire probes are used in the cold wire mode or, more precisely, the constant current, low overheat ratio mode. The wires used on the aircraft and on the balloons are only slightly heated by the current flowing through the wire. Consequently, the wire seeks an equilibrium temperature determined by conservation of energy. At low velocity in a nonreacting flow, the probe temperature is only slightly higher than the ambient, freestream air temperature, also called the static temperature. At higher velocities, the probe, or in fact any temperature sensor, responds to the combination of the thermal energy in the flow (static temperature) and the organized kinetic energy of the flow relative to the sensor. This phenomenon is sometimes known as dynamic heating or the compressibility effect.

This problem is usually analyzed in terms of the equilibrium temperature that an adiabatic surface will achieve. This adiabatic wall temperature, or recovery temperature,[11] is defined by

$$T_r = T + r\left(U^2 \big/ 2C_p\right) \tag{2}$$

The recovery factor r is equal to unity at the stagnation point, where all of the kinetic energy is converted to heat, and the recovery temperature is the stagnation temperature or the total temperature. As one moves along the body downstream of the stagnation point, the recovery factor gets smaller; it can become zero or even slightly negative on the leeward side of a body.[12]

The wire on a sensing probe is very long compared to its diameter, so that conduction along the wire length is slight except near the ends. Even without longitudinal conduction, the wire does conduct heat through the cross section, so that one can define an average recovery factor for a given cross-sectional geometry. Measured values of the average value of r for a thin cylindrical wire depend on Mach number.[13] [Note that Ref. 13 does not present a recovery factor, but instead the ratio of equilibrium (recovery) temperature to total temperature.] The values tend to be greater than or equal to the recovery factor for a flat plate, which is the square root of the Prandtl number (for air, $Pr = 0.7$, and so $r = 0.84$).

As we will show, when the flow is fast enough, fluctuations of either ambient temperature or velocity can cause a fluctuation in recovery temperature. If velocity fluctuation terms become significant, then the velocity fluctuation contribution must be removed to determine the actual air temperature fluctuation so that fluctuations in index of refraction, the optical turbulence, can be computed. The methods for obtaining the fluctuations in velocity in a compressible flow were derived by Morkovin[14] and have continued to be refined (for a recent example, see work by Nagabushana et al.[15]). Typically at least two wires are used. At least one of the wires is used in the constant temperature mode with a high overheat ratio, and typically two or more equations must be solved simultaneously to determine the fluctuations in air temperature and velocity. Clearly, the correction for velocity is not required for low Mach numbers, but above a certain Mach number, it becomes significant. The addition of another wire at a different overheat condition, the additional calibration and data acquisition requirements, and the coupled solution of equations for very large data sets, make the decision to correct for velocity fluctuation measurements a serious matter.

This paper examines the consequences of not correcting for velocity fluctuations on the apparent optical turbulence as a function of increasing velocity and estimates this error using actual atmospheric data. We also estimate the impact of the error on computed optical performance. We hope to approach the topic in a way that can be appreciated by atmospheric scientists interested in optical turbulence as well as aeronautical engineers.

Theory

Introduction to Theory

In this section, we first present the coordinate system used to examine the problem. We give particular attention to relating standard coordinates used to express the mean and fluctuating components of the wind to the body-fixed coordinates used to examine the airflow around a sampling airplane. Next, we relate fluctuations in air temperature and velocity to recovery temperature fluctuations sensed by a sensor on a sampling airplane. Next, we perform a formal statistical treatment of the fluctuations in measured recovery temperature by first calculating the spatial covariance of the measured term. The resulting terms are associated with covariances and cross covariances in temperature and velocity. Next, the equation is simplified based on order of magnitude arguments, and the equation is converted to both variance form and spectral form. Finally, the spectral form is analyzed and estimates are made of the individual terms.

Coordinates

The U^2 in Eq. (2) is the dot product of the vector $\boldsymbol{U}$, the velocity of the air relative to the temperature-sensing instrument with itself. Refer to Fig. 1 for the vectors used in the analysis. Consider the aircraft moving with a velocity $\boldsymbol{V}_{gs}$ relative to the ground. The plane is moving through a wind field of velocity $\boldsymbol{V}_w$ characterized by the mean and fluctuating components

$$\boldsymbol{V}_w = (\bar{u} + u')\hat{\boldsymbol{i}} + (\bar{v} + v')\hat{\boldsymbol{j}} + (\bar{w} + w')\hat{\boldsymbol{k}} \tag{3a}$$

where the velocities are defined relative to the ground. For convenience, the wind vector is shown as the sum of mean and fluctuating parts:

$$\boldsymbol{V}_w = \bar{\boldsymbol{V}}_w + \boldsymbol{V}'_w \tag{3b}$$

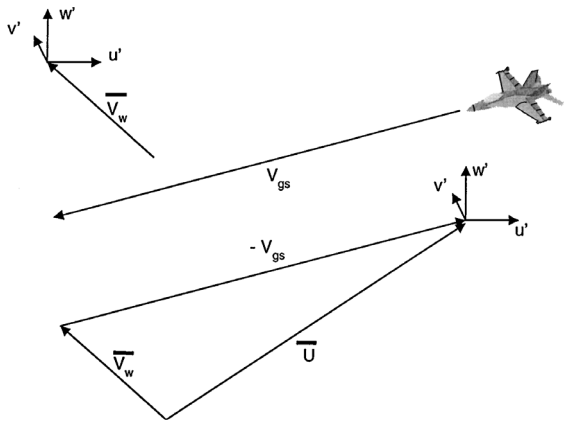

Fig. 1 Vectors used in the equations: V_{gs} is the velocity vector of the aircraft relative to the ground; V_w the wind velocity vector, composed of a mean wind speed with the bar, and fluctuating components u', v', and w'; and U (not shown) is the true air speed vector and is the sum of the mean value $\bar{U}$ plus the fluctuating wind components.

The true air speed velocity vector $\boldsymbol{U}$ is determined by subtracting the aircraft velocity, assumed constant, from the wind velocity:

$$\boldsymbol{U} = \boldsymbol{V}_w - \boldsymbol{V}_{\text{gs}} \tag{4a}$$

Performing the indicated operations, we have

$$\boldsymbol{U} = \bar{\boldsymbol{V}}_w - \boldsymbol{V}_{\text{gs}} + \boldsymbol{V}'_w \tag{4b}$$

Next we define the mean true air speed vector $\bar{\boldsymbol{U}}$ as the mean wind velocity minus the ground speed vector:

$$\bar{\boldsymbol{U}} = \bar{\boldsymbol{V}}_w - \boldsymbol{V}_{\text{gs}} \tag{5}$$

The result is that the true air speed vector is the mean true air speed vector $\bar{\boldsymbol{U}}$ plus the fluctuating components of the wind velocity vector:

$$\boldsymbol{U} = \bar{\boldsymbol{U}} + \boldsymbol{V}'_w \tag{6}$$

In the lower part of Fig. 1, the fluctuating components have been moved over to the end of the $\bar{\boldsymbol{U}}$ vector. The instantaneous true air speed (not shown) is a vector that extends from the tail of the $\bar{\boldsymbol{U}}$ vector to the head of the fluctuating part of the wind vector.

Now, performing the dot product

$$\begin{aligned} U^2 = \boldsymbol{U}\cdot\boldsymbol{U} &= (\bar{\boldsymbol{U}} + \boldsymbol{V}'_w)\cdot(\bar{\boldsymbol{U}} + \boldsymbol{V}'_w) \\ &= \bar{U}^2 + 2(\bar{\boldsymbol{U}}\cdot\boldsymbol{V}'_w) + V'^2_w \\ &= \bar{U}^2 + 2\bar{U}U' + V'^2_w \end{aligned} \tag{7}$$

For simplification, we use the symbol U' for the component of the fluctuating wind velocity in the mean true air speed direction, which is defined by the equation

$$U' = (\bar{\boldsymbol{U}}\cdot\boldsymbol{V}'_w)/|\bar{\boldsymbol{U}}| \tag{8}$$

By convention, the magnitude of $\bar{\boldsymbol{U}}$ is always positive, but U' will be positive or negative depending on the direction of $\boldsymbol{V}'_w$, relative to $\bar{\boldsymbol{U}}$. If the fluctuating component of the wind at an instant in time were such that the sign of U' were positive, then if the sensor had been moving in the opposite direction, the sign of U' would have been negative at that instant. Note that, for horizontal flight and no significant mean vertical component of wind, fluctuating vertical wind components will not contribute to this term.

Fluctuations in Recovery Temperature

The primary concern of the majority of the compressible flow anemometry literature is the determination of velocity fluctuation in the face of the contaminating temperature fluctuations. The emphasis here is just the opposite, the contamination of the temperature fluctuation measurement by velocity fluctuations.

Assuming that the measured temperature is essentially the recovery temperature, we proceed to compute the mean of the recovery temperature. Assume that we are in a homogeneous region where the aforementioned mean values of the velocities are steady and the mean of the fluctuating parts is zero. Further, air temperature is expressed as the sum of a mean and a fluctuating part:

$$T = \bar{T} + T' \tag{9}$$

Substituting Eqs. (7) and (9) into Eq. (2), we have

$$T_r = \bar{T} + T' + (r/2C_p)\left[\bar{U}^2 + 2\bar{U}U' + V'^2_w\right] \tag{10}$$

For a homogeneous region, the mean recovery temperature is

$$\bar{T}_r = \bar{T} + (r/2C_p)\bar{U}^2 + (r/2C_p)\bar{V}'^2_w \tag{11}$$

Subtracting Eq. (11) from Eq. (10), we obtain the fluctuating part of the recovery temperature

$$T'_r = T' + (r\bar{U}U'/C_p) + (r/2C_p)\left(V'^2_w - \bar{V}'^2_w\right) \tag{12}$$

Next we calculate the spatial covariance of the measured temperature, $B_{Tr}(x)$ that is defined as[16]

$$\begin{aligned} B_{T_r}(x_2 - x_1) &= \langle (T_r(x_1) - \langle T_r(x_1)\rangle)(T_r(x_2) - \langle T_r(x_2)\rangle)\rangle \\ &= \langle T_r(x_1)T_r(x_2)\rangle - \langle T_r(x_1)\rangle\langle T_r(x_2)\rangle \end{aligned} \tag{13}$$

where we have denoted time averages by the symbols $\langle\ \rangle$ to avoid confusion.

For a stationary, homogeneous random process, the mean value of recovery temperature at a point is constant, which we can write as $\langle T_r\rangle$, and the covariance depends only on the magnitude of $x = (x_2 - x_1)$. To simplify the notation, we shall use the subscript 1 and 2 to denote the location x_1 and x_2:

$$B_{T_r}(x) = \langle T_{r1}T_{r2}\rangle - \langle T_{r1}\rangle\langle T_{r2}\rangle \tag{14}$$

Now substituting Eqs. (10) and (11) into Eq. (14) yields

$$\begin{aligned} B_{T_r}(x) = {} & \langle T'_1T'_2\rangle + (r\bar{U}/C_p)\langle T'_1U'_2 + T'_2U'_1\rangle \\ & + \left(r^2\bar{U}^2/C_p^2\right)\langle U'_1U'_2\rangle + (r/2C_p)\left\langle T'_1V'^2_{w2} + T'_2V'^2_{w1}\right\rangle \\ & + \left(r^2\bar{U}/2C_p^2\right)\left\langle U'_1V'^2_{w2} + U'_2V'^2_{w1}\right\rangle + \left(r^2/4C_p^2\right)\left\langle V'^2_{w1}V'^2_{w2}\right\rangle \\ & - \left(r^2/4C_p^2\right)\left\langle V'^2_{w1}\right\rangle\left\langle V'^2_{w2}\right\rangle \end{aligned} \tag{15}$$

We can identify these various terms with covariances and cross covariances, namely,

$$\begin{aligned} B_{T_r}(x) = {} & B_T(x) + (r\bar{U}/C_p)[B_{T,U}(x) + B_{U,T}(x)] \\ & + \left(r^2\bar{U}^2/C_p^2\right)B_U(x) + (r/2C_p)\left[B_{T,V_w^2}(x) + B_{V_w^2,T}(x)\right] \\ & + \left(r^2\bar{U}/2C_p^2\right)\left[B_{U,V_w^2}(x) + B_{V_w^2,U}(x)\right] + \left(r^2/4C_p^2\right)B_{V_w^2}(x) \end{aligned} \tag{16}$$

Note that the primes have been dropped from the subscripts of the covariance and cross-covariance symbols, which, by definition, [Eq. (13)] are measures of the fluctuations. Using the property of covariances that $B_{xy}(\tau) = B_{yx}(-\tau)$ for real x and y, Eq. (16) becomes

$$\begin{aligned} B_{T_r}(x) = {} & B_T(x) + (r\bar{U}/C_p)[B_{T,U}(x) + B_{T,U}(-x)] \\ & + \left(r^2\bar{U}^2/C_p^2\right)B_U(x) + (r/2C_p)\left[B_{T,V_w^2}(x) + B_{T,V_w^2}(-x)\right] \\ & + \left(r^2\bar{U}/2C_p^2\right)\left[B_{U,V_w^2}(x) + B_{U,V_w^2}(-x)\right] + \left(r^2/4C_p^2\right)B_{V_w^2}(x) \end{aligned} \tag{17}$$

This is the final, formal expression that also explicitly includes and specifies the higher-order terms (HOT) and moments. Note that in SI units, C_p is on the order of 10^3 for air, so that terms with U/C_p can only become significant as U becomes large. Terms without

velocity probably remain quite small, except for the temperature term. Rewriting the significant terms of Eq. (17), we have

$$B_{T_r}(x) = B_T(x) + (r\bar{U}/C_p)[B_{T,U}(x) + B_{T,U}(-x)] + \left(r^2\bar{U}^2/C_p^2\right)B_U(x) + \text{HOT} \quad (18)$$

By evaluating Eq. (18) at $x = 0$, we have the relationship between the variances:

$$\overline{T_r'^2} = \overline{T'^2} + 2(r\bar{U}/C_p)\overline{U'T'} + (r\bar{U}/C_p)^2\bar{U}'^2 + \text{HOT} \quad (19)$$

The B_T and B_U terms of Eq. (18) are even by inspection of Eq. (14). The sum of the positive and negative sides of the $B_{T,U}$ function is clearly an even function. The Fourier transformation of Eq. (18) yields the relation of the recovery temperature spectrum in terms of the atmospheric temperature and longitudinal wind spectrum and the temperature–wind cospectrum:

$$S_{T_r} = S_T(k) + 2(r\bar{U}/C_p)S_{UT}(k) + (r\bar{U}/C_p)^2 S_U(k) + \text{HOT} \quad (20)$$

Note that the primes are reinstated in the variance equation, but are not used in the spectral expression, because it is clear that we are looking at fluctuations over a range of wave numbers k.

The next task at hand is to determine the relative magnitudes of the terms. At this point, it is worthwhile to discuss the origin of temperature fluctuations (see Ref. 17 or any fluid mechanics text that treats turbulence). The essence of turbulence is fluctuations in flow velocity. In the presence of temperature gradients, the fluctuations in flow velocity produce fluctuations in fluid temperature. Because the temperature of a parcel of fluid tends to change with changes in pressure due to the work of expansion, meteorologists use the thermodynamic variable potential temperature θ defined by the equation[18]

$$\theta = T(P_s/P)^{(\gamma-1)/\gamma} \quad (21)$$

where P_s is a reference pressure, usually 1×10^5 Pa, that is nearly the standard pressure at mean sea level. The potential temperature is the temperature achieved by a parcel of air that is adiabatically compressed or expanded to the reference pressure from a given state P and T. For a given pressure, the ratio of the structure constants C_T^2 to C_θ^2 is equal to the ratio of T^2/θ^2.

For a fluid in a turbulent state, gradients of potential temperature determine if velocity fluctuations will produce temperature fluctuations. It is very possible to have velocity turbulence with very little fluctuation in temperature. In fact, turbulence itself tends to mix fluid parcels of different potential temperature, which, eventually, reduces temperature fluctuations while velocity fluctuations persist at high levels.

For purposes of obtaining an analytical result, we will focus on turbulence in an equilibrium state. This ignores the initial period before the turbulence cascade is established and the final decay period, when turbulence levels are too small to matter. At equilibrium, Kolmogorov hypothesized that turbulent kinetic energy cascades from the largest eddies, called the outer scale of the turbulence, to the smallest eddies, the inner scale, primarily by inertial processes.[19] At the inner scale, kinetic energy is converted to thermal energy by viscous dissipation. By virtue of the Kolmogorov hypothesis, small-scale isotropy is also implied. When the velocity spectrum is within the inertial range (between the outer and inner scale), a result of the Kolmogorov hypothesis is that the one-way, one-dimensional power spectral density of longitudinal velocity fluctuations has the following functional relationship[20]:

$$S_U(k) = 0.25C_U^2 k^{-\frac{5}{3}} \quad (22)$$

(Note that in the inertial range, the second-order cross-stream and vertical components of velocity structure functions in the longitudinal direction[20] are larger by a factor of $\frac{4}{3}$.)

Obhukov[21] and Corrsin[22] showed that, for the size range that temperature fluctuations are dominated by velocity fluctuations, the spectra should follow a similar relationship, that is,

$$S_T(k) = 0.25C_T^2 k^{-\frac{5}{3}} \quad (23)$$

There is analysis and experimental evidence[23–25] that the velocity–temperature cospectrum does not enjoy the same functional relationship with k, and so it will be left as an unspecified function of wavelength:

$$S_{T_r} = (0.25)C_T^2 k^{-\frac{5}{3}} + (r\bar{U}/C_p)^2(0.25)C_U^2 k^{-\frac{5}{3}} + (2r\bar{U}/C_p)S_{UT}(k) + \text{HOT} \quad (24)$$

Now, combining the terms with like power of wave number and dropping HOT the recovery temperature spectrum is

$$S_{T_r}(k) = (0.25)\left[C_T^2 + \left(r^2\bar{U}^2/C_p^2\right)C_U^2\right]k^{-\frac{5}{3}} + (2r\bar{U}/C_p)S_{UT}(k) \quad (25)$$

Velocity–Temperature Cospectral Term

We consider the term that contains the variance of the $U'T'$ product in Eq. (19) or the cospectrum of velocity and temperature fluctuations in Eq. (25). We assume that U' is horizontal, which is typical for sampling missions. This term can be either positive or negative because the sign of U' is determined by the direction of flight. Some observations can be made about the contribution of this term. 1) If we are examining a collection of many data runs flown in opposite directions, the contribution of this term should not affect the mean of the collected data, although it will increase the variance of the data set. 2) Although strong correlation of velocity and temperature fluctuations is expected when caused by gravity waves at large scales, there may be low correlation of the two in the inertial range of isotropic turbulence. The cross correlation of horizontal velocity and temperature is the basis for horizontal turbulent heat flux. This is significant when there are strong temperature gradients in the positive or negative U' direction, but horizontal temperature gradients are usually very weak compared to vertical gradients. The strongest gradients, which are associated with fronts,[26] are only of the order 10^{-5} K/m. 3) Finally, by the Schwartz inequality, the magnitude of the term is bounded by the magnitude of the product of the individual components U' and T'. Therefore, in times of low temperature fluctuation, the cross term must also have a low value. For these reasons, we conclude that this term is not important when looking at differences in the mean of collections of data from different directions, nor can it be important when the temperature variance is small.

Velocity and Temperature Spectral Terms

Setting aside the cospectral term, the problem now is to determine the relative magnitudes of C_T^2 and C_U^2, to substitute the magnitudes into Eq. (25), and to determine the relative significance. The grouping shown in Eq. (25) suggests that the velocity structure constant, which is never negative, adds to the recovery temperature spectrum throughout the inertial range in a way that is indistinguishable from temperature fluctuations. For purposes of comparison, we extract the temperature structure constant from the combined temperature and velocity term to yield

$$C_T^2\left[1 + \left(r^2\bar{U}^2/C_p^2\right)\left(C_U^2/C_T^2\right)\right]$$

We will refer to the term in the brackets as the velocity contamination factor that amplifies the actual temperature structure constant by the uncorrected velocity fluctuation. A plot of the velocity contamination factor is shown in Fig. 2 for air speeds up to 300 m/s and values of the ratio of the velocity and temperature structure constants up to 100. As shown in Fig. 2, the need to correct for velocity fluctuation depends on the sensor velocity, the desired accuracy of the measurement, and the value of the ratio of the structure constants. In the next section, we present a discussion of measured and estimated values of the structure constants.

Magnitudes of the Structure Constants

Temperature Structure Constant

Consider first the temperature structure constant. The procedure used to convert balloon-borne instrument data to the temperature structure constant assumes the Kolmogorov result[2] that

$$D_T(d) = C_T^2 d^{\frac{2}{3}} \quad (26)$$

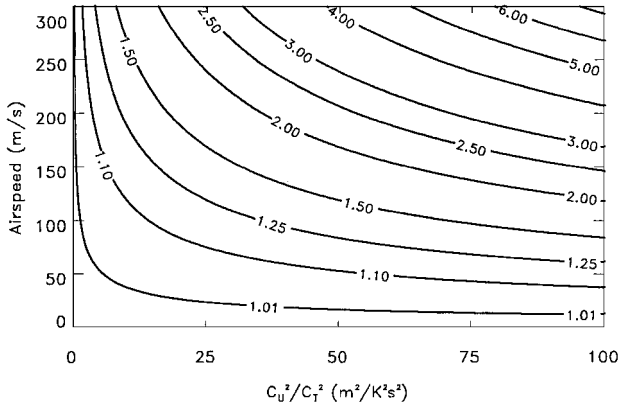

Fig. 2 Velocity contamination factor for air speeds up to 300 m/s and ratios of the spectral constants (velocity to temperature) from 0 to 100; assumed value of the recovery factor r is 0.84.

where d is the distance between the points of measurement and $D_T(d)$ is the structure function. As shown in Fig. 2, the temperatures measured by the balloon-borne sensors at the relatively low ascent velocity of 5 m/s do not suffer from velocity contamination effects. The balloon acquires temperature differences at a 1-m separation; therefore, the magnitude of the 1-m structure function, $D_T(1\text{ m})$, is the magnitude of the structure constant. The amplitude of balloon acquired temperature structure constant C_T^2 typically varies from the Thermosonde noise floor (1×10^{-6}–1×10^{-5} $K^2/m^{2/3}$) to a maximum of around 0.01 $K^2/m^{2/3}$. Values below 1×10^{-5} $K^2/m^{2/3}$ do not significantly affect optical propagation. Conversion of the temperature structure constant to the refractive index structure constant C_n^2 depends on local pressure and temperature and the wavelength of the radiation that is being propagated. For radiation near the visible spectrum, it is customary to use the formula[2]

$$C_n^2 = (79 \times 10^{-8} P/T^2) C_T^2 \tag{27}$$

Velocity Structure Constant

Velocity fluctuations have been measured over the years. They are often reported in terms of the turbulent kinetic energy dissipation rate ε, which by virtue of the Kolmogorov hypothesis is[2]

$$C_U^2 = a\varepsilon^{\frac{2}{3}} \tag{28}$$

where a is a dimensionless constant that was determined to be approximately 2–3 from measurements in the free atmosphere. We have used a value of 2 for this analysis.

Aircraft Measurements

Values of ε from aircraft measurements[27,28] range from 1×10^{-5} m^2/s^3 in very quiet air to a high value of almost 0.1 m^2/s^3 in severe storms. The transition from negligible turbulence to low turbulence is roughly 3×10^{-3} m^2/s^3, and, in fact, the occurrences of turbulence above this value are infrequent.

Radar Measurements

There are two methods used to determine ε using radar data. One method uses the Doppler spectral spreading of the return beam and the other uses a relationship of C_n^2, the gradient Richardson number, and the Brunt–Väisälä frequency, which are defined subsequently.[29] The second method suffers from the necessity to estimate the fraction of the atmosphere that is turbulent and the requirement to rely on available balloon soundings to determine the gradient Richardson number and the Brunt–Väisälä frequency. The two methods are in general agreement, and the values of ε range from a low of 1×10^{-7} m^2/s^3 to a high of 0.1 m^2/s^3.

Balloon Measurements

Values of ε can also be inferred from the data products of the Thermosonde[28] using an extension of the second radar method just mentioned. In fact, the computation of ε from the Thermosonde eliminates the shortcomings of the comparable radar calculation. First, the response of the instrument is fast enough to eliminate the need to estimate the turbulent fraction of the atmosphere (it is unity). Second, the atmospheric sounding data are taken concurrently with the C_T^2 data. In addition, the calculation for the Thermosonde does not require terms that include the contribution of water vapor to the index of refraction for radar wavelengths. The theoretical basis for the method comes from the relation (Ref. 3, pp. 67–74)

$$C_\theta^2 = a_\theta \chi \varepsilon^{-\frac{1}{3}} \tag{29}$$

where a_θ is a numerical constant determined by experiment[30] to be approximately 3.2. If the turbulence is stationary, the dissipation rate of temperature fluctuations χ is in turn also related to ε by the relation[31]

$$\chi = b\varepsilon(\nabla\bar{\theta})^2/N^2 \tag{30}$$

where N is the Brunt–Väisälä frequency defined by

$$N^2 = \frac{g}{\bar{\theta}} \frac{\mathrm{d}\bar{\theta}}{\mathrm{d}z} \tag{31}$$

A value of $\frac{1}{3}$ was used in this study for the parameter b. This is representative[32] for a Richardson number greater than $\frac{1}{4}$, which is valid over most of the flight. The gradient Richardson number, defined by the equation

$$Ri = N^2 \Big/ \left(\frac{\mathrm{d}\bar{V}_w}{\mathrm{d}z}\right)^2 \tag{32}$$

is a measure of the stability of the atmosphere. A value of Richardson number less than approximately $\frac{1}{4}$ is an indication that the atmosphere is unstable and turbulence can be initiated by the wind shear (Ref. 18, p. 461). Because b is often reduced for smaller values of Richardson number,[28] our calculation for ε is conservative. Assuming the vertical component of the potential temperature gradient is the primary contribution to the total gradient of potential temperature in Eq. (30), we can solve for ε using the equation

$$\varepsilon = \left[\frac{g\bar{\theta} C_T^2}{a_\theta b T^2 (\mathrm{d}\bar{\theta}/\mathrm{d}z)}\right]^{\frac{3}{2}} \tag{33}$$

When this method is used with balloon data, the computed values of ε range from a low of 1×10^{-7} m^2/s^3 to a rare high of 0.1 m^2/s^3.

Summary

By any of the aforementioned methods to measure ε, the values range from very low values of 1×10^{-7} m^2/s^3 to a rare high of 0.1 m^2/s^3. Values up to 1×10^{-3} m^2/s^3 are common. Using Eq. (28), the estimated values of C_U^2 range from a low value of 1×10^{-3} $m^{4/3}/s^2$ to a high of 0.4 $m^{4/3}/s^2$, with common occurrences up to 0.02 $m^{4/3}/s^2$.

Results

Unfortunately, the preceding estimation of the range of values for the structure constants of velocity and temperature does not really capture the effect of the velocity contamination. It is not the occurrence of moderately high value of velocity fluctuation alone, but the combined occurrence of high velocity fluctuation and low temperature fluctuation that causes a large velocity contamination factor. Hypothetical ratios constructed from maximum values of C_U^2 and minimum values of C_T^2 are misleading. A realistic estimate requires ratios based on simultaneous measurements in the atmosphere. To capture this combined effect, we use the method described to obtain ε and C_U^2 from the balloon measured atmospheric conditions including C_T^2. We applied this technique to data from five balloon ascents over the White Sands Missile Range (WSMR), New Mexico, in September 1997. Of 11 ascents made in that campaign, 5 flights were selected because they had nearly complete data coverage throughout most of the flight. The methodology is demonstrated using data from flight number 4 (Fig. 3) that resulted in a modest amount of velocity contamination when projected to a high-speed temperature sensor.

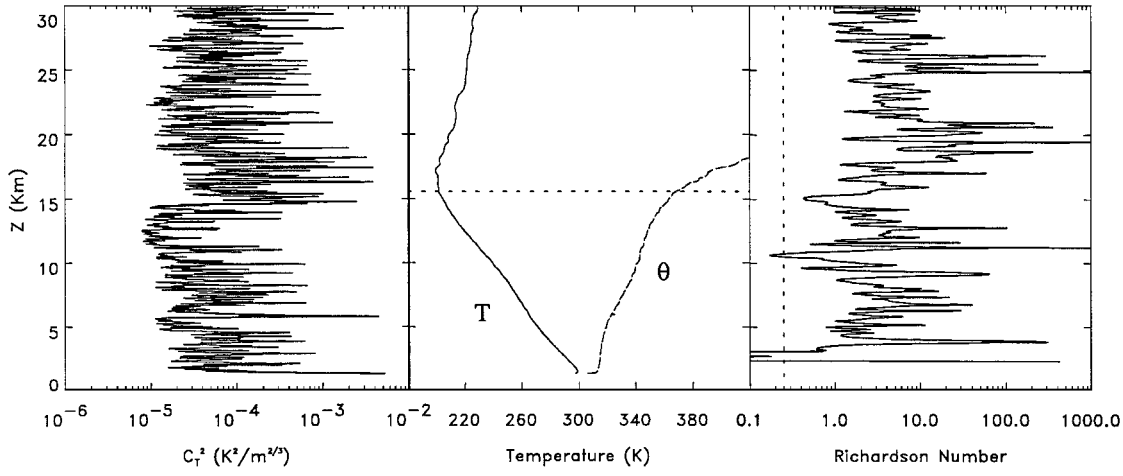

Fig. 3 Profile of temperature structure constant, temperature (——) and potential temperature (- - - -), and Richardson number, for altitudes from 2 km up to nearly 30 km (plotted on the ordinate).

The primary variables for the calculations are shown in Fig. 3. On the left-hand side of Fig. 3 is the C_T^2 for each altitude. This flight has a noise floor of approximately 10^{-5} $K^2/m^{2/3}$. The mean temperature profile is shown in the center. The horizontal dotted line denotes the tropopause, which is the maximum altitude of generally decreasing temperatures of the troposphere. Also shown with the dashed line is the potential temperature profile for the lower altitudes, computed using Eq. (21). Potential temperature generally increases slowly in the troposphere, then increases more rapidly in the stratosphere, above the tropopause. The gradient of potential temperature is used in the calculation of Richardson number and ε.

The Richardson number profile is shown on the right-hand side of Fig. 3. The dotted line is for $Ri = 0.25$, the critical number for the Kelvin–Helmholtz instability. This profile indicates a range of very low Richardson number from 2 to 4 km reflecting the nearly zero gradient of potential temperature in that range, indicating a region of instability. For regions with Richardson number above 1, any turbulence would be in a state of decay.[28]

The predicted velocity turbulence, expressed in terms of turbulent kinetic energy dissipation ε is shown in on the left-hand side of Fig. 4. Note that we have narrowed the altitude range from 10 to 15 km, the altitudes of interest for the aircraft sampling. The range of ε looks reasonable. Our predicted minimum is restricted by the noise floor of the temperature fluctuation instrument. The veracity of the very thin spikes with high ε is still under study. More interesting are the deeper regions of moderate levels, indicating regions of velocity turbulence.

The ratio of the velocity structure constant to the temperature structure constant that is required to compute the velocity contamination factor is actually independent of the measured value of the temperature structure constant. By manipulation of Eqs. (28–30), evaluation of the constants, and use of the definition of potential temperature, we obtain

$$\frac{C_U^2}{C_T^2} \approx \frac{\varepsilon}{\chi} \approx \frac{3g}{\theta}\left(1 \Big/ \frac{\mathrm{d}\theta}{\mathrm{d}z}\right) \tag{34}$$

On the left-hand side of Fig. 5, we show the profile of the ratio of the structure constants. One obvious characteristic is the dramatic difference in the behavior relative to the tropopause. As we pass through the tropopause region and enter the stratosphere, the increasing values of both the potential temperature and its gradient strongly suppress the large excursions in ratio that are evident in the troposphere. A second feature is the number of regions of very high ratios of nearly 1 km or less in depth.

On the right-hand side of Fig. 5, we show the profile of the estimated velocity contamination factor for an aircraft flying at 200 m/s based on data from the balloon flight described earlier. We see the expected similarity to the behavior of the structure constant ratio.

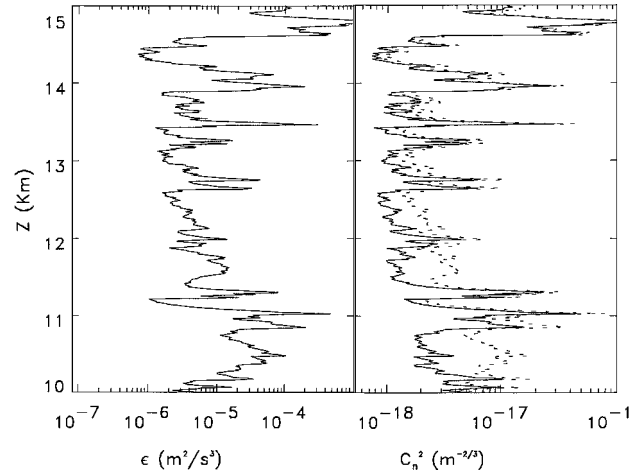

Fig. 4 Predicted velocity turbulence expressed as dissipation of turbulent kinetic energy ε: right, profiles of refractive index structure constant, the actual value, and the estimated uncorrected value; ——, C_n^2 determined by the balloon; and · · · ·, estimate of the perceived C_n^2 for a probe traveling at 200 m/s.

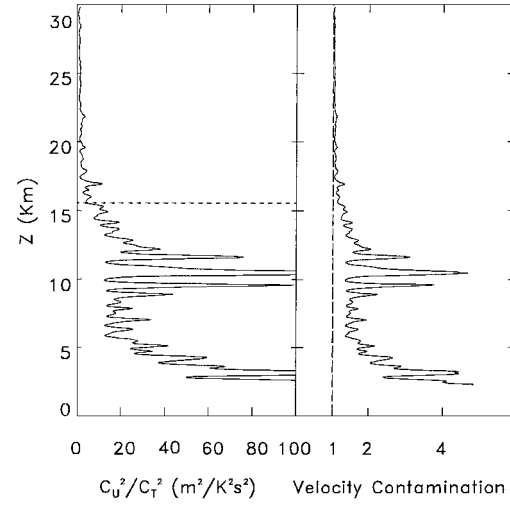

Fig. 5 Left, profile of the ratio of the velocity structure constant to the temperature structure constant: – – –, tropopause; right, profile of the estimated velocity contamination factor for an aircraft flying at 200 m/s.

This result implies that it may not be necessary to correct for velocity fluctuations when sampling well into the stratosphere. However, this may be an artifact of the combination of thinner turbulence layers in the stratosphere and slower response of the mean temperature sensor in the lower density of the upper atmosphere. Therefore, we would like to reserve judgment until faster mean temperature sensors are used.

The velocity contamination factor is the ratio of the structure constant of fluctuations of uncorrected temperature to actual temperature, ignoring the cospectral term. At any given altitude, this ratio is the same value as the ratio of the respective index of refraction structure constants. On the right-hand side of Fig. 4, we show two profiles of the refractive index structure constant, the actual value and the estimated value without a velocity correction, for typical altitudes of airborne sampling (10–15 km). The solid line is the C_n^2 determined by the balloon; the dotted line is our estimate of the perceived C_n^2 for a probe traveling at 200 m/s. The actual amount of contamination varies with altitude, reflecting the underlying variation in atmospheric conditions. Whereas the mean amplification over the region of 10–15 km is less than a factor of 2, some local maxima are observed that are well above the mean. The largest amplification ratios occur in regions where actual C_n^2 is low. Local maxima in the actual C_n^2 profile often bound regions of high values of ε, such as the regions from 10 to 12 km and from 11.5 to 12 km. In some regions of low C_n^2, the amplification is also low, which must be interpreted as regions of very low turbulence.

Comparison to Other Research

Are the regions of high velocity turbulence and low temperature turbulence indicated by our measurements substantiated by other research? There have been only a few reports of concurrent turbulent velocity and temperature fluctuation measurements in the upper troposphere and the stratosphere. Barat and Bertin[33] reported ratios of C_U^2 to C_T^2 of 10 often and, in one instance, of 40 in the center of a large billow. Note that a factor of 40 would only double the perceived optical turbulence of an airborne probe moving at 200 m/s; however, their measurements were in the stratosphere. At low altitudes, in the atmospheric boundary layer, ratios of 500 and above have been measured.[34]

Recent direct numerical simulation studies of breaking gravity waves[35] have, at least qualitatively, demonstrated these phenomena. The simulation shows strong velocity and temperature variance at early stages of the development of the turbulent region (or billow). As the billow matures, there is a decrease of temperature gradients in the center of the billow that results in a decrease in temperature fluctuations even though velocity fluctuations persist throughout the turbulent layer for a much longer time.

Optical Performance Calculations

Our principal interest in optical turbulence is the effect that C_n^2 has on the computation of optical performance. There are many different measures of optical performance. One simple measure of the turbulence effects on imaging is the path integral of C_n^2 that appears in the calculation of the transverse coherence length and Fried's coherence length for plane waves.[2] An increased value of the line integral indicates an increase to the optical degradation caused by the turbulence.

For this study, we have taken a vertical path integral of C_n^2 from 10 to 15 km, which could be used to determine the impact on a vertical propagation path between the two altitudes. The comparison of the integrals of actual and perceived C_n^2 with limits from 10 to 15 km for the five WSMR profiles is shown in Table 1. These results indicate that if uncorrected data were used from a temperature probe moving at 200 m/s, one would predict optical degradation of from 50 to 80% worse than the actual optical degradation, for the conditions of the WSMR campaign.

It is more difficult to estimate the overprediction of beam degradation for propagation paths that are nearly horizontal. First, a horizontal path is really a tangent for a spherical Earth, and so a beam of modest length does not stay at the same altitude for a very long distance. Next, we do not know the horizontal extent of the layers, and so long extrapolations are questionable. Last, because the starting altitude of the propagation is probably arbitrary within a possible range, there is only a calculable probability that propagation will occur in the layer that is experiencing a high value of velocity amplification. On the average, the mean effect on any optical path in the region is the mean of the contamination factor over the range of operating altitudes. Therefore, the ratio shown in Table 1 is, conveniently, the mean value that one might expect in the overestimation of optical degradation with uncorrected data at the time and place that these data were acquired.

Table 1 Comparison of the integral of the actual C_n^2 profile to the integral of the C_n^2 profile as perceived by a temperature probe moving at 200 m/s

Flight number	Integral C_n^2, $m^{1/3} \times 10^{14}$, 10–15 km	Integral of perceived C_n^2, 10–15 km	Ratio of perceived to actual
3	1.29	2.25	1.74
4	2.73	4.27	1.56
5	0.67	1.04	1.55
7	1.27	2.31	1.81
10	1.90	2.87	1.51

Conclusion

An analysis of the expected fluctuation of sensor temperature given fluctuations in both temperature and velocity shows that the effects of the velocity fluctuations appear in two terms that can become significant as velocity increases. The term that includes the velocity variance is always a positive contribution to the sensor temperature fluctuations. The results of this analysis show that even moderate levels of velocity turbulence can contribute significantly to the perceived levels of temperature fluctuations and, consequently, index of refraction fluctuations if not corrected. The contribution is most significant in regions that have low temperature fluctuations and high velocity fluctuations. The contribution from the second term involving velocity, the velocity–temperature covariance, can be either positive or negative, depending on direction of flight, and is limited by the magnitudes of the individual variances. Therefore, for a collection of samples flown back and forth over a ground track, the term should not contribute significantly to the mean of the perceived optical turbulence, but would tend to spread the range of measured values. The contribution of the cross term is not expected to be large when the actual temperature turbulence fluctuations are small.

When there is low temperature turbulence, it can be due to either low values of velocity turbulence or the presence of strong velocity turbulence that has mixed the fluid well enough to reduce the gradient of potential temperature. In the latter case, the moving sensor will perceive large temperature fluctuations when, in fact, they are small. This phenomenon is the natural result of turbulent mixing in the atmosphere. In these cases, uncorrected aircraft derived optical turbulence levels are significantly higher than actual levels.

Data from five balloon ascents were used to estimate the value of the uncorrected optical turbulence from an aircraft in the high troposphere flying at 200 m/s. The result was that the inferred optical degradation would be 50–80% too high for that region at the time of the balloon ascents. These data also indicate that the effect of velocity fluctuations is stronger in the troposphere than the stratosphere; however, this could be an artifact of mean temperature measurement devices that are too slow to measure the thinner turbulence layers in the stratosphere.

We recommend the techniques presented to researchers who are trying to determine the need for a velocity fluctuation sensor in the instrument suite of aircraft performing optical turbulence measurements.

Acknowledgments

The authors are indebted to John B. Wissler, who developed the velocity contamination expression using the variance approach and made early estimates of its magnitude. He and Demos Kyrazis helped us develop the complete form of the equations and offered many valuable suggestions for this work.

References

[1]Owens, J. C., "Optical Refractive Index of Air: Dependence on Pressure, Temperature and Compositions," *Applied Optics*, Vol. 6, No. 1, 1967, pp. 51–59.

[2]Beland, R. R., "Propagation Through Atmospheric Optical Turbulence," *The Infrared and Electro-Optical Systems Handbook*, Vol. 2, *Atmospheric Propagation of Radiation*, edited by F. G. Smith, Infrared Information Analysis Center, Ann Arbor, MI, and SPIE Optical Engineering Press, Bellingham, WA, 1993, pp. 157–132.

[3]Tatarski, V. I., *The Effects of the Turbulent Atmosphere on Wave Propagation*, TT-68-50464, National Technical Information Service, Springfield, VA, 1971.

[4]Ierkic, H. M, Woodman, R. F., and Perillat, P., "Ultrahigh Vertical Resolution Radar Measurements in the Lower Stratosphere at Arecibo," *Radio Science*, Vol. 25, No. 5, 1990, p. 941.

[5]Brown, J. H., Good, R. E., Bench, P. M., and Faucher, G., "Sonde Measurements for Comparative Measurements of Optical Turbulence," Air Force Geophysics Lab., AFGL-TR-82-0079, ADA118740, National Technical Information Service, Springfield, VA, 1982.

[6]Jumper, G. Y., Polchlopek, H. M., Beland, R. R., Murphy, E. A., Tracy, P., and Robinson, K., "Balloon-Borne Measurements of Atmospheric Temperature Fluctuations," AIAA Paper 97-2353, June 1997.

[7]Otten, L. J., "Airborne Observations of Tropopausal Turbulence," AIAA Paper 85-0342, Jan. 1985.

[8]Otten, L. J., Pavel, A. L., Finley, W. E., and Rose, W. C., "A Survey of Recent Atmospheric Turbulence Measurements from a Subsonic Aircraft," AIAA Paper 81-0298, Jan. 1981.

[9]Rose, W. C., and Otten, L. J., "Airborne Measurement of Atmospheric Turbulence," *Aero-Optical Phenomena*, edited by K. G. Gilbert and L. J. Otten, Vol. 80, Progress in Astronautics and Aeronautics, AIAA, New York, 1982, pp. 325–337.

[10]Eaton, F. D., Nastrom, G. D., Masson, B., Hahn, I., McCrae, K., Nowlin, S. R., and Berkopec, T., "Radar and Aircraft Observations of a Layer of Strong Refractivity Turbulence," *Airborne Laser Advanced Technology*, edited by T. D. Steiner and P. H. Merritt, Vol. 3381, SPIE Proceedings, Society for Photo-Optical Instrumentation Engineers, Bellingham, WA, 1998, pp. 230–238.

[11]White, F. M., *Heat and Mass Transfer*, Addison–Wesley, Longman, MA, 1988, pp. 358–361.

[12]Eckert, E. R. G., and Drake, R., *Heat and Mass Transfer*, McGraw–Hill, New York, 1959, pp. 255–267.

[13]Laufer, J., and McClellan, R., "Measurement of Heat Transfer from Fine Wires in Supersonic Flows," *Journal of Fluid Mechanics*, Vol. 1, 1956, pp. 276–289.

[14]Morkovin, M. V., "Fluctuations and Hot-Wire Anemometry in Compressible Flows," AGARDograph 24, 1956.

[15]Nagabushana, K. A., Stainback, P. C., and Jones, G. S., "A Rational Technique for Calibrating Hot-Wire Probes in Subsonic to Supersonic Speeds," AIAA Paper 94-2536, June 1994.

[16]Gottman, J. M., *Time-Series Analysis*, Cambridge Univ. Press, Cambridge, England, UK, 1981, p. 67.

[17]Schlichting, H., "Fundamentals of Turbulent Flow," *Boundary-Layer Theory*, McGraw–Hill, New York, 1968, pp. 521–559.

[18]Kundu, P. K., *Fluid Mechanics*, Academic, New York, 1990, pp. 20, 461.

[19]Kolmogorov, A. N., "The Local Structure of Turbulence in Incompressible Viscous Fluid for Very Large Reynolds Numbers," *Doklady Akademii Nauk SSSR (Soviet Physics—Doklady)*, Vol. 30, No. 4, 1941, p. 229.

[20]Paquin, J. E., and Pond, S., "The Determination of the Kolmogoroff Constants for Velocity, Temperature and Humidity Fluctuations from Second- and Third-Order Structure Functions," *Journal of Fluid Mechanics*, Vol. 50, Pt. 2, 1971, pp. 257–269.

[21]Oboukhov, A. M., "Structure of the Temperature Field in Turbulent Flows," *Izvestiya Akademii Nauk SSR, Serizy Geograficheskaya i Geofizicheskaya*, Vol. 13, No. 1, 1949, p. 58.

[22]Corrsin, S., "On the Spectrum of Isotropic Temperature Fluctuations in Isotropic Turbulence," *Journal of Applied Physics*, Vol. 25, 1951, p. 657.

[23]Lumley, J. L., "The Spectrum of Nearly Inertial Turbulence in a Stably Stratified Fluid," *Journal of Atmospheric Sciences*, Vol. 21, No. 1, 1964, pp. 99–102.

[24]Wyngaard, J. C., and Cote, O. R., "Cospectral Similarity in the Atmospheric Surface Layer," *Quarterly Journal of the Royal Meteorological Society*, Vol. 98, No. 417, 1972, pp. 590–603.

[25]Kaimal, J. C., Wyngaard, J. C., Izumi, Y., and Cote, O. R., "Spectral Characteristics of Surface Layer Turbulence," *Quarterly Journal of the Royal Meteorological Society*, Vol. 98, No. 417, 1972, pp. 563–689.

[26]Rao, G. V., "On the Influences of Fields of Motion, Baroclinicity and Latent Heat Source on Frontogensis," *Journal of Applied Meteorology*, Vol. 5, No. 4, 1966, p. 377.

[27]Trout, D., and Panofsky, H. A., "Energy Dissipation Near the Tropopause," *Tellus*, Vol. 21, No. 3, 1969, pp. 355–358.

[28]Hocking, W. K., and Mu, P. K. L., "Upper and Middle Tropospheric Kinetic Energy Dissipation Rates from Measurements of C_n^2—Review of Theories, *in-situ* Investigations, and Experimental Studies Using the Buckland Park Atmospheric Radar in Australia," *Journal of Atmospheric and Solar-Terrestrial Physics*, Vol. 59, No. 14, 1997, pp. 1779–1803.

[29]Cohn, S. A., "Radar Measurements of Turbulent Eddy Dissipation Rate in the Troposphere: A Comparison of Techniques," *Journal of Atmospheric and Oceanic Technology*, Vol. 12, No. 1, 1995, pp. 85–95.

[30]Wyngaard, J., and LeMone, M., "Behavior of the Refractive Index Structure Parameter in the Entraining Convective Boundary Layer," *Journal of Atmospheric Sciences*, Vol. 37, No. 7, 1980, pp. 1573–1585.

[31]Weinstock, J., "Vertical Turbulent Diffusion in a Stably Stratified Fluid," *Journal of Atmospheric Sciences*, Vol. 35, No. 6, 1978, pp. 1022–1027.

[32]Lilly, D., Waco, D., and Adelfang, S., "Stratospheric Mixing Estimated from High-Altitude Turbulence Measurements," *Journal of Applied Meteorology*, Vol. 13, No. 4, 1974, pp. 488–493.

[33]Barat, J., and Bertin, F., "Simultaneous Measurements of Temperature and Velocity Fluctuations Within Clear Air Turbulence Layers: Analysis of the Estimate of Dissipation Rate by Remote Sensing Techniques," *Journal of Atmospheric Sciences*, Vol. 41, May 1984, p. 1613.

[34]Hunt, J. C. R., Kaimal, J. C., and Gaynor, J. E., "Some Observations of Turbulence Structure in Stable Layers," *Quarterly Journal of the Royal Meteorological Society*, Vol. 111, No. 469, 1985, pp. 793–815.

[35]Werne, J., and Fritts, D. C., "Stratified Shear Turbulence: Evolution and Statistics," *Geophysical Research Letters*, Vol. 26, No. 4, 1999, pp. 439–442.

J. P. Gore
Associate Editor